

Comparison of In Vivo Optical Systems for Bioluminescence and Fluorescence Imaging

Steven K. Cool · Koen Breyne · Evelyne Meyer ·
Stefaan C. De Smedt · Niek N. Sanders

Received: 23 August 2011 / Accepted: 4 April 2012 / Published online: 12 April 2013
© Springer Science+Business Media New York 2013

Abstract In vivo optical imaging has become a popular tool in animal laboratories. Currently, many in vivo optical imaging systems are available on the market, which often makes it difficult for research groups to decide which system fits their needs best. In this work we compared different commercially available systems, which can measure both bioluminescent and fluorescent light. The systems were tested for their bioluminescent and fluorescent sensitivity both in vitro and in vivo. The IVIS Lumina II was found to be most sensitive for bioluminescence imaging, with the Photon Imager a close second. Contrary, the Kodak system was, in vitro, the most sensitive system for fluorescence imaging. In vivo, the fluorescence sensitivity of the systems was similar. Finally, we examined the added value of spectral unmixing algorithms for in vivo optical imaging and demonstrated that spectral unmixing resulted in at least a doubling of the in vivo sensitivity. Additionally, spectral unmixing also enabled separate imaging of dyes with overlapping spectra which were, without spectral unmixing, not distinguishable.

Keywords Optical imaging · In vivo · Bioluminescence · Fluorescence · Spectral unmixing

S. K. Cool · N. N. Sanders (✉)
Laboratory of Gene Therapy, Department of Nutrition, Genetics and Ethology, Faculty of Veterinary Medicine, Ghent University, Merelbeke 9820, Belgium
e-mail: Niek.Sanders@UGent.be

S. K. Cool · S. C. De Smedt
Laboratory of General Biochemistry and Physical Pharmacy, Department of Pharmaceutics, Faculty of Pharmaceutical Sciences, Ghent University, Ghent 9000, Belgium

K. Breyne · E. Meyer
Laboratory of Biochemistry, Department of Pharmacology, Toxicology and Biochemistry, Faculty of Veterinary Medicine, Ghent University, Merelbeke 9820, Belgium

Introduction

In vivo optical imaging is a non-invasive imaging technique that pictures and reveals molecular and biological processes using bioluminescent and fluorescent reporters and/or probes. It is a powerful tool for monitoring and tracking cells, gene expression, new drug compounds, metabolites, pathogens, etc. in living animals. Consequently, in vivo optical imaging is used extensively on small animals in the fields of diagnostics [1–4], disease development and -progress [5–7], drug discovery & development [2, 8–11] and functional genomics [12]. In the future, it could even be used to aid tumor resection surgery in superficial tissues; like breast-conserving surgery [13]. The success of this technology is attributed to its high sensitivity, high temporal resolution, high throughput capacities, ease of use and excellent cost-effectiveness. This in contrast to other, non-optical imaging techniques, like radiography, ultrasound, magnetic resonance imaging (MRI), computed- (CT) and positron emission tomography (PET), which have a higher tissue penetration, but often lack contrast and high temporal resolution. Additionally, functional studies are not straightforward with the latter techniques and they are often less safe, more expensive and labor-intensive. Nevertheless, in vivo optical imaging has also drawbacks and one of them is the limited penetration of light through tissues. This is due to scattering and absorbance of light by tissues. Additionally, tissue auto-fluorescence further complicates in vivo optical fluorescent imaging [14]. However, these problems associated with in vivo optical imaging have partly been solved by the introduction of near-infrared (NIR) fluorescent probes [15, 16]. Indeed, the scattering and absorbance of light by tissues reaches a minimum at wavelengths between 700 nm and 900 nm. Additionally, the autofluorescence of tissues is also lower in the NIR. A further new development in the field of in vivo optical imaging is the combination with other, structural, imaging modalities, like MRI or CT [9].

The performance of an in vivo optical imaging system is largely dependent on the quality of the charge coupled device (CCD) camera, which is the heart of every optical imaging system. When evaluating different systems, it is best to compare some of the features of the CCD camera. A back-thinned, back-illuminated CCD is designed to have an increased photon absorption, enhancing the quantum efficiency of the CCD and the sensitivity of the system. A second important parameter of a CCD is its dark current, i.e. the ‘signal’ generated in absence of light. It is the charge that leaks into a pixel during the exposure time in the absence of light. This readout noise is the limiting factor in low-light images, as is often the case with bioluminescent imaging. Dark current can be limited in two ways. One possibility is to cool the camera. CCD cameras are cooled to $-29\text{ }^{\circ}\text{C}$ or $-90\text{ }^{\circ}\text{C}$, depending on the CCD chip design, to obtain a sufficiently low dark current. A second possibility to reduce dark current is the use of a cooled intensifier tube, which intensifies incoming signal-photons by a factor of 10^6 before they reach the CCD. This means that dark current is no longer an issue, as it is not intensified. Binning is often used to increase the sensitivity of a CCD. It is the mathematical combination of pixels to one computed ‘pixel’. Binning results in an increase of the dynamic range and sensitivity, however, it reduces the spatial resolution.

The lens, which is positioned before the CCD, is also of importance in in vivo optical imaging. The two most important parameters of any optical lens are the focal length and its minimal and maximal aperture (diameter of the diaphragm). The focal length of a lens is defined by the distance between the middle of the lens and the focal point. The ratio of the focal length to the pupil diameter of the aperture defines the focal ratio, or *f*/number (Eq. 1).

$$f/\text{number} = \left(\frac{\text{focal length}}{\text{pupil diameter}} \right) \quad (1)$$

Notice that the *f*/number is inversely proportional to the pupil diameter of the aperture. On modern lenses, the *f*/number can usually only be adjusted in discrete steps. These are then called *f*/stops and in general each *f*/stop differs from the previous *f*/stop by a factor that equals the square root of two. Hence, the theoretical possible *f*/stops of a lens are given by the following sequence: $f/(\sqrt{2})^n$, with $n=0,1,2,3,4, \dots$. A decrease of one *f*/stop implies, based on Eq. 1, that the diameter of the pupil increases with $\sqrt{2}$. As the pupil of a lens is more or less circular its surface equals $\pi \times \left(\frac{\text{diameter}}{2}\right)^2$. Therefore, when the *f*/stop is decreased with one step the surface of the pupil of the aperture will double and hence allow that a double amount of light can reach the CCD camera. Consequently, to push an optical imaging system

to its maximum sensitivity one should use the lowest possible *f*/stop.

When using fluorescence imaging, the choice of the appropriate emission and excitation filters are of major importance. Therefore, to evaluate an in vivo optical imaging system, one should check both the available filters and check how easy it is to interchange them. The bandpass of the filters is of critical importance when working with multiple probes. The narrower the bandpass of excitation and emission filters, the better the system can detect multiple dyes and differentiate between the spectra of the dyes and background auto-fluorescence. Spectral unmixing is an additional tool to resolve different fluorophores with overlapping spectra by excitation- or emission-based unmixing of these fluorophores. Spectra unmixing makes use of an algorithm that can distinguish the spectral signatures of different fluorescent dyes or bioluminescent reporters and calculate the respective contribution of each on every pixel of an image [17].

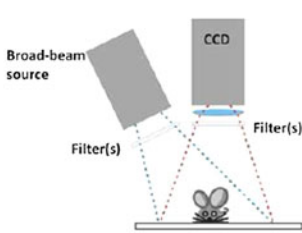
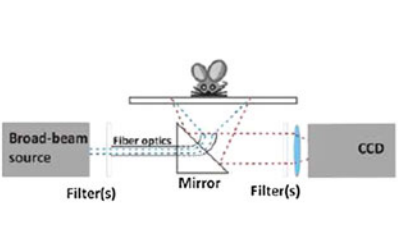
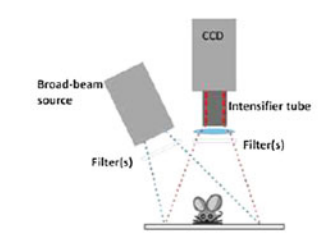
Finally, an integrated gas anesthesia system and a heating system to support the body temperature of the animals are also crucial.

Materials and Methods

Instrumentation

The IVIS Lumina II is designed for both bioluminescent (BLI) and fluorescent imaging (FLI). For FLI, light coming from a tungsten halogen lamp is guided through one of 10 possible excitation filters. The animals are top illuminated by the excitation light as illustrated in Table 1. The emitted fluorescent light is subsequently filtered by one of 4 broad band-pass emission filters present in the standard filter wheel. The standard filter wheel can be replaced by 4 other possible filter wheels each containing 7 emission filters with a narrow bandpass of 20 nm. For this study the narrow bandpass emission filters were used. For BLI, the light produced by the luciferase catalyzed reaction within the animals is guided through an open position present in the emission filter wheel. The fluorescent light or the bioluminescent light is subsequently collected by a *f*/95–*f*/16 lens mounted on a back-thinned, back-illuminated, 1024×1024 pixels, 16 bit CCD camera which is thermoelectrically cooled with a Peltier element to $-90\text{ }^{\circ}\text{C}$. The minimal detectable radiance of the camera is $100\text{ photons/s/sr/cm}^2$, where sr stands for steradian, which is the SI unit of solid angle. It is used to describe two-dimensional angular spans in three-dimensional space. More detailed specifications on the lens and CCD camera are shown in Table 1, which gives a side-by-side comparison of the technical aspects of the tested systems. The field of view (FOV) can be adjusted to either: $5 \times 5\text{ cm}$, $7.5 \times 7.5\text{ cm}$, $10 \times 10\text{ cm}$ or $12.5 \times 12.5\text{ cm}$ by

Table 1 Comparison of some of the most important characteristics of the three in vivo optical imaging systems

Scheme showing the key components of the three compared systems			
Excitation source	Halogen lamp	Xenon lamp	Halogen lamp
Excitation filters (nm)	430, 465, 500, 535, 570, 605, 640, 675, 710, 745	Automated and customizable filter wheel	Continuous from 400 nm to 800 nm by 5 nm steps with 20 nm bandwidth
Emission filters (nm)	Standard series filter wheel: 515-575, 575-650, 695-770, 810-875 500, 600 and 700 series filter wheel: 500 nm to 740 nm in 20 nm steps	Filters of choice between 420 nm and 850 nm	6 high-pass filters: 530, 570, 615, 660, 700, 770 (others available upon request)
Lens (f/number)	f/9.5 - f/16	f/2 - f/32	f/1.4 - f/22
Min. and max field of view (FOV) (cm)	5x5, 7x7, 10x10, 12.5x12.5	Continuous from: 2x2 to 20x20	Continuous from: 8x6 to 24x18
CCD Size Imaging pixels Pixel size (µm) Min. detectable radiance Operating temperature	Back-thinned, back-illuminated 1.69 cm ² 1024x1024 13 100 ph/s/sr/cm ² -90 °C	Monochrome interlined CCD Available upon request Available upon request Available upon request -29 °C	Intensified CCD 0.5 cm ² (photocathode = 1.5 cm ²) 1042x1042 7.4 75ph/s/sr/cm ² Room temperature
Software	Living image 3.1	Available upon request	Photo vision and M ³ Vision

lowering the imaging stage. At the highest FOV up to three mice can be imaged at once. There is an accessory lens available, with a maximal FOV of 24 × 24 cm, which allows simultaneous imaging of five mice. Image analysis and spectral unmixing was performed by the living image 3.1 software from CaliperLS.

The *Photon Imager* (see Table 1) is capable of real-time bioluminescent and fluorescent in vivo imaging and also of imaging of non-anaesthetized animals with an optional module. A halogen lamp generates light which is filtered through a continuous linear filter, which makes it possible to select 20 nm wide bands of wavelengths between 400 and 800 nm, with a 5 nm precision. The photon imager uses the following six high pass filters for filtering the emission light: 530 nm, 570 nm, 615 nm, 660 nm, 700 nm and 770 nm. This type of emission filter makes it impossible to spectral unmix certain combinations of emission spectra. In this paper the in vivo images generated with the Photon imager were corrected for auto-fluorescence. The system does this automatically by taking an additional image of the animal using excitation light with a wavelength that is 50 nm shorter than the one used for the signal acquisition. Subsequently, this background image was subtracted from the original image. A f/1.4 - f/22 lens with computer-controlled zoom, allowing for a continuous FOV from 8 × 6 cm to 24 × 18 cm is used to capture the emitted light. The Photon imager uses a cooled intensifier tube that amplifies

the original photon signal by a factor 10⁶ making CCD cooling redundant. Due to this amplification the Photon Imager has a temporal resolution of 20 ms which enables the user to perform kinetic studies, as signal accumulation is displayed in real-time. The weakest detectable radiance is 75 photons/s/sr/cm². The system uses the Photo Vision software for acquiring and the M³Vision software for analyzing and manipulating images.

The *Kodak Image Station* can image both bioluminescent and fluorescent signals. This system uses a xenon lamp as illumination source. For FLI, light passes through an excitation filter and is projected via fiber optics through the optical transparent table on which the animal is positioned (bottom illumination). The setup is outlined in Table 1. Fluorescent light is collected through the optical transparent table and guided by a 45° high efficiency mirror through an emission filter. The instrument contains a four-insert filter wheel, which can hold emission filters of choice between 420 and 850 nm, plus an open position for BLI. The filtered emission light is collected through an f/2 - f/32, 10x automatic zoom lens which guides the light to a thermoelectrically cooled (-29 °C) CCD camera.

Animals

Ten weeks old female nude mice (NMRI^{Nu/Nu}) were purchased from Janvier Breeding Center (Le Genest St. Isle,

France). Animals were anaesthetized with an intraperitoneal (i.p.) injection of 0.1 ml/10 g of an isotonic solution containing 10 mg/ml ketamine and 1 mg/ml xylazine. The experiments were approved by the ethical committee of the Faculty of Veterinary Medicine (Ghent University; EC2010/002).

Liposomes

Liposomes contained 55 mol% DPPC (dipalmitoylphosphatidylcholine), 5 mol % DSPE-PEG-Biotin (1,2-distearoyl-*sn*-glycero-3-phosphoethanolamine-polyethylene glycol₂₀₀₀-biotin), 39 mol % cholesterol and either 1 mol % DiD (1,1-dioctadecyl-3,3,3',3'-tetramethylindodicarbocyanine perchlorate) (Invitrogen, USA) or 1 mol% DiR (1,1-dioctadecyl-3,3,3,3-tetramethylindotricarbocyanine iodide) (AnaSpec, USA). DPPC, DSPE-PEG-Biotin and cholesterol were purchased from Avanti Polar Lipids (Alabaster, USA). DiD and DiR are lipophilic fluorescent tracers that stably insert in lipid (bi)layers. The emission and excitation spectra of DiD and DiR inserted in phospholipid bilayer membranes are shown in Fig. 1a. We prepared the liposomes via the evaporation/hydration method. Lipids, dissolved in chloroform, were mixed in a round-bottomed flask. Subsequently, the chloroform was evaporated at 37 °C using a rotavapor. The resulting lipid film was rehydrated using 4-(2-hydroxyethyl)-1-piperazineethanesulfonic acid (HEPES) buffer (20 mmol/l HEPES, pH 7.4) at a final lipid concentration of 5 mg/ml. The obtained suspension is extruded 10 times through a 100 nm pore polycarbonate filter membrane using a mini-extruder (Avanti Polar Lipids). The resulting liposome suspension contained 224nM fluorescent dye.

Fluorescence Imaging

In Vitro Sensitivity A serial dilution (using 3-fold dilution steps) of the fluorescent labeled liposomes was prepared in triplicate in a black 96-well plate (Greiner Bio-One,

Belgium) using HEPES buffered glucose (20 mM HEPES, 5 % glucose, pH 7.4). The concentration of the DiD and DiR labeled liposomes ranged between 224 nM and 4 pM DiR or DiD. As a background, we used the fluorescent signal measured in wells containing only the HEPES buffered glucose.

In Vivo Sensitivity Four concentrations of DiD-liposomes (0.224 nM, 0.0448 nM, 0.0112 nM and 0.0056 nM) and HEPES buffered glucose were mixed 1:1 with matrigel (BD Biosciences, Belgium). 200 µl of these mixtures was injected subcutaneously (s.c.) in five spots on the dorsal side with a 26G needle (Fig. 3a). The 1:1 mixture of HEPES buffered glucose and matrigel was injected in the middle of the back and served as a negative control. Matrigel was used to increase the viscoelasticity of the dispersions and hence to retain the injected liposomes as much as possible within the injected area. This mouse was used as a standard to compare all three systems.

For the spectral unmixing experiments we also used, besides living mice, the XMF-2 Fluorescent phantom mouse (CaliperLS) in which we inserted rostrally a rod containing Alexa750 and caudally a rod with 850 nm quantum dots (QD850). The spectra of these fluorescent dyes are shown in Fig. 1b. Spectral unmixing was performed with the spectral unmixing algorithm on the IVIS lumina II.

Several images were taken with each system and representative images are shown in Figs. 2 and 3. The generated pictures show as much signal as possible for each system separately, while showing as little background as possible.

Bioluminescence Imaging

In Vitro Sensitivity To determine the bioluminescence sensitivity of the instruments we made a serial dilution of a stock suspension of bioluminescent *Escherichia coli* (*E. coli* XEN14, Caliper Life Sciences) containing 1.5×10^6 CFU

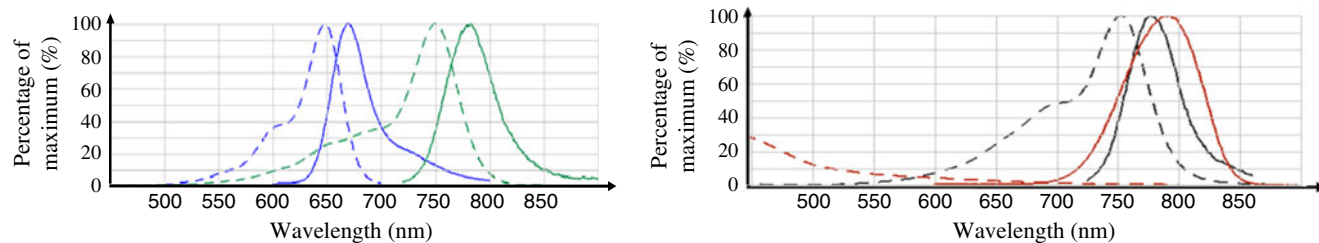


Fig. 1 A. Excitation (dotted lines) and emission (full lines) spectra of DiD (blue) and DiR (green) bound to phospholipid bilayer membranes. The excitation maxima of DiD and DiR are around 650 nm and 750 nm, while their emission maxima are around 670 nm and 780 nm, respectively (Source: Invitrogen Fluorescence SpectraViewer). B. Excitation (dotted lines) and emission (full lines) spectra of AF750

(black) and QD800 (red). The excitation maximum of AF750 is around 750 nm, while the excitation peak of QD800 is elongated from around 300 nm to 700 nm. Their emission maxima are very similar, i.e. around 780 nm, (Source: Invitrogen Fluorescence SpectraViewer)

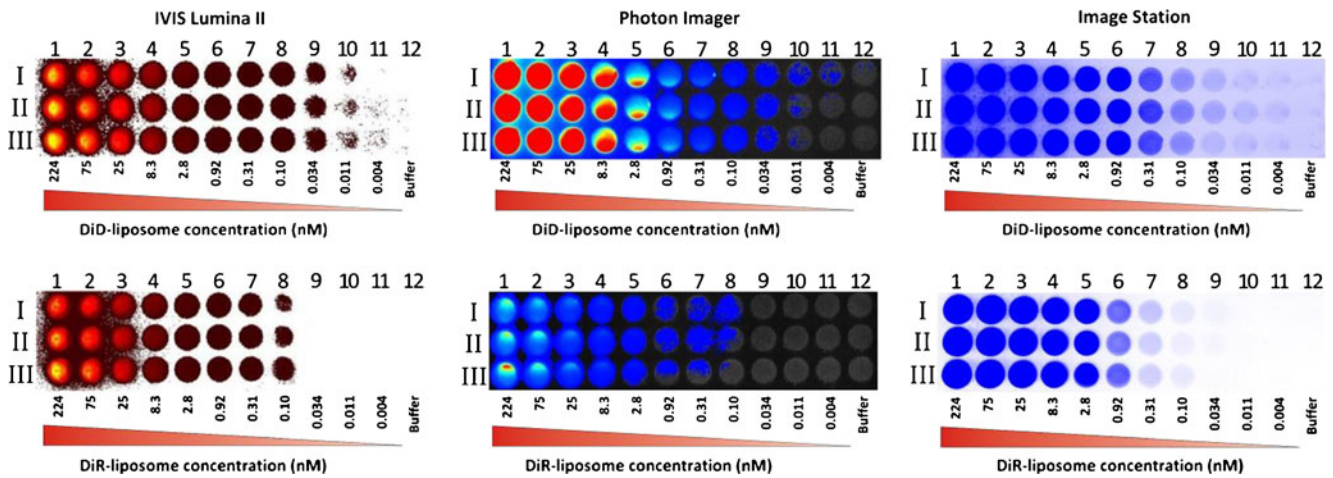


Fig. 2 In vitro fluorescence sensitivity of the optical imaging systems. Three serial dilution of DiD-liposomes (*top row*) and DiR-liposomes (*bottom row*) were prepared in black 96-well plates (*rows I, II, III*) and imaged with the three optical imaging systems. The concentration in each row decreased from left to right. The images of the DiD-liposomes were taken using the following settings; *IVIS Lumina II*: f/stop 2, exposure time 1 s, binning 2×2 , filters $\lambda_{\text{ex}}=640 \text{ nm}/\lambda_{\text{em}}=720 \text{ nm}$; *Photon Imager*: f/stop 1.8, exposure time 4 s, filters $\lambda_{\text{ex}}=610 \text{ nm}/\lambda_{\text{em}}=$

660 nm ; *Image Station*: f/stop 2.5, exposure time 60s, binning 2×2 , filters $\lambda_{\text{ex}}=630 \text{ nm}/\lambda_{\text{em}}=700 \text{ nm}$. The images of the DiR-liposomes were taken using the following settings; *IVIS Lumina II*: f/stop 2, exposure time 10s, binning 1×1 , filters $\lambda_{\text{ex}}=745 \text{ nm}/\lambda_{\text{em}}=820 \text{ nm}$; *Photon Imager*: f/stop 2, exposure time 10s, filters $\lambda_{\text{ex}}=720 \text{ nm}/\lambda_{\text{em}}=770 \text{ nm}$; *Image Station*: f/stop 2.5, exposure time 60s, binning 2×2 , filters $\lambda_{\text{ex}}=730 \text{ nm}/\lambda_{\text{em}}=790 \text{ nm}$

(colony forming units) per ml. Out of this stock suspension we prepared nine different *E. coli* concentrations in black 96-well plates using magnesium free PBS (Invitrogen): 0, 10, 100, 1000, 1500, 1.5×10^4 , 1.5×10^5 , and 1.5×10^6 CFU per 100 μl . As background we used the average bioluminescent signal coming from two wells containing 100 μl PBS.

In Vivo Sensitivity Four different bacteria suspensions containing 225×10^4 , 225×10^3 , 225×10^2 , 2250 CFU in

100 μl PBS were mixed 1:1 with matrigel. 100 μl of these mixtures was s.c. injected in four spots on the dorsal side with a 26G needle. The number of bacteria per injection spot was: 1.125×10^6 , 1.125×10^5 , 1.125×10^4 and 1125. In the centre of the back, 100 μl of a 1:1 mixture of PBS and matrigel was injected as a negative control. This mouse was used as a standard to compare all three systems.

Several images were taken with each system and representative images are shown in Figs. 6 and 7. The

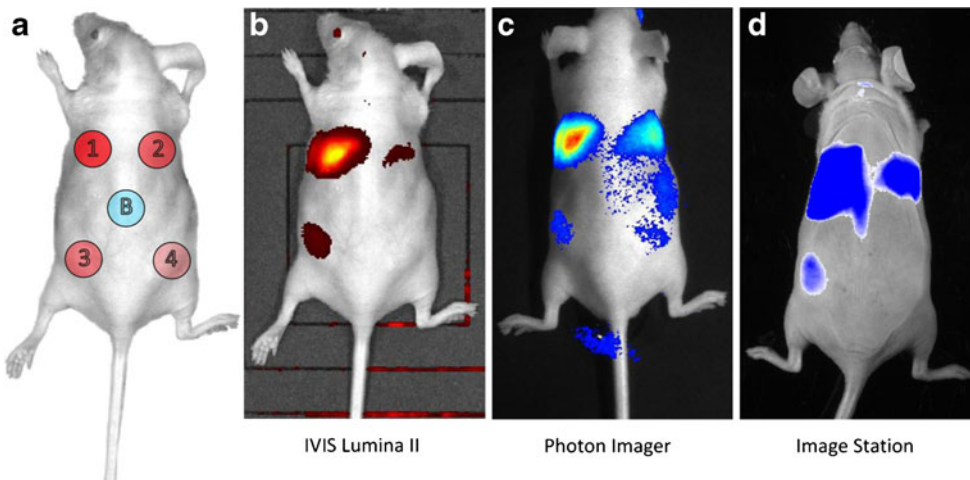


Fig. 3 In vivo fluorescence sensitivity and image quality of the tested optical imaging systems. Mixtures containing decreasing DiD-liposome concentrations in matrigel were injected subcutaneously in four different spots on the dorsal side. The location of these injections is shown in scheme **a**. The concentration of the DiD-liposomes in spot 1, 2, 3 and 4 were 112 pM, 22.4 pM, 5.6 pM and 2.8 pM, respectively. In spot (**b**) a mixture of buffer and matrigel was injected. Images **b**, **c**

and **d** show the same mouse imaged by the three evaluated systems. The image were taken using the following settings; *IVIS Lumina II*: f/stop 2, exposure time 1 s, binning 4×4 , filters $\lambda_{\text{ex}}=640 \text{ nm}/\lambda_{\text{em}}=720 \text{ nm}$; *Photon Imager*: f/stop 1.4, exposure time 9 s, filters $\lambda_{\text{ex}}=610 \text{ nm}/\lambda_{\text{em}}=660 \text{ nm}$; *Image Station*: f/stop 2.51, exposure time 60s, binning 4×4 , filters $\lambda_{\text{ex}}=630 \text{ nm}/\lambda_{\text{em}}=700 \text{ nm}$. The image of the Photon Imager was obtained after background subtraction.

generated pictures show as much signal as possible for each system separately, while showing as little background as possible.

Results

In this paper we performed a side-by-side comparison of in vivo optical imaging systems that are designed for both fluorescence imaging (FLI) and bioluminescence imaging (BLI) of small animals. The following three instruments were tested: (1) IVIS Lumina II (CaliperLS, USA), (2) Photon Imager (Biospace lab, France), and (3) Image Station (Kodak, USA). These instruments are so-called planar imaging systems that generate a 2D fluorescence or bioluminescence image that can be overlaid with a photographic image of the animal. The sensitivity of the instruments and the quality of the images were checked in vitro and in living mice using fluorescent probes and bioluminescent bacteria. Furthermore, the added value of spectral unmixing algorithms was evaluated with the IVIS Lumina II.

Fluorescence Imaging Capabilities

In Vitro Sensitivity

An important parameter of an in vivo optical imaging system is its sensitivity. To evaluate the fluorescence sensitivity of the instruments we made three serial dilutions of DiD and DiR labeled liposomes in black 96-well plates. The liposome concentrations were varied between 224 nM and 4 pM DiD or DiR and the total volume in the wells was kept constant at 100 μ L. The well plates were imaged with each instrument using the most optimal settings. The selected settings are mentioned in the legend of Fig. 2. We defined the *visible detection limit* as the lowest concentration that was visible in all three dilution series. The obtained images of the dilutions series are shown in Fig. 2. With the IVIS Lumina II, the Photon Imager and the Image Station, the visible detection limits of the DiD-liposomes were 11 pM, 11 pM and 4 pM, respectively. The detection limits of the DiR-liposomes were much higher and equalled 100 pM, 100 pM and 34 pM (very weak signal, only visible on the screen) in the IVIS Lumina II, the Photon Imager and the Image Station, respectively.

In Vivo Sensitivity and Image Quality

In vivo FLI is, in contrast to in vitro experiments, complicated by tissue autofluorescence as well as scattering and absorbance of light. Therefore, we also evaluated the in vivo fluorescence sensitivity of the three instruments. Four different DiD-liposome concentrations were mixed 1:1 with

matrigel and subcutaneously injected in separated spots on the dorsal side of a mouse. Figure 3a depicts the location of the injection spots. A 1:1 mixture of buffer and matrigel was injected in between the four spots and served as a negative control. The mice were imaged with the settings, mentioned in the legend of Fig. 3. The IVIS Lumina II and the Image Station were able to detect the three highest concentrations. In contrast, all four spots could be seen with the Photon imager. However, the fluorescence signal from the lowest concentration was extremely weak and not well distinguishable from the spot above. Consequently, a person who is not aware of the experimental design would most likely not consider this spot as a positive signal. Therefore, we concluded that the lowest detectable concentration of the DiD-liposomes was 5.6 pM in all three instruments.

Advantages of Spectral Unmixing

Spectral unmixing software was available on the IVIS Lumina II and the Image Station. The spectral unmixing software of the Image Station was a beta-version at the time of the experiments. Therefore, we decided to evaluate the advantages of spectral unmixing using the IVIS Lumina II.

To evaluate whether the spectral unmixing algorithm allows for separate imaging of dyes with overlapping spectra we equipped the XFM-2 phantom mouse with two rods which contain at their ends Alexa Fluor 750 (AF750) and Quantum dots 850 (QD850), respectively (Fig. 1b). As shown in Fig. 4b, it is impossible to image AF750 without also detecting QD850. This is due to the broad excitation peak of QD850 and the similar emission spectra of AF750 and QD850 (Fig. 1b). Subsequently, we determined whether these dyes can be separated via spectrum unmixing. Therefore, different images of the phantom mouse were made using the following filter combinations: excitation filters 605 nm, 640 nm, 675 nm, 710 nm and 745 nm in combination with emission filter 800 nm. The spectral unmixing software uses the information in these images to estimate the excitation spectra of AF750 and QD850, and to calculate the contribution of AF750 and QD850 to the total fluorescence measured in each pixel. Figure 4b–d clearly demonstrate that the spectral unmixing algorithm can separate both dyes and hence confirms there is actually no AF750 present in the lower rod. Similar results can be obtained by using the Image Station's excitation based spectral unmixing algorithm (data not shown).

The added value of spectral unmixing was further demonstrated using a mouse injected with four different DiD-liposomes concentrations (Fig. 5). Four images of the mouse, each taken with a different excitation and emission filter combination ($\lambda_{\text{ex}}=640$ nm and $\lambda_{\text{em}}=720$ nm, 740 nm, 760 nm, 780 nm), were constructed by the instrument. These

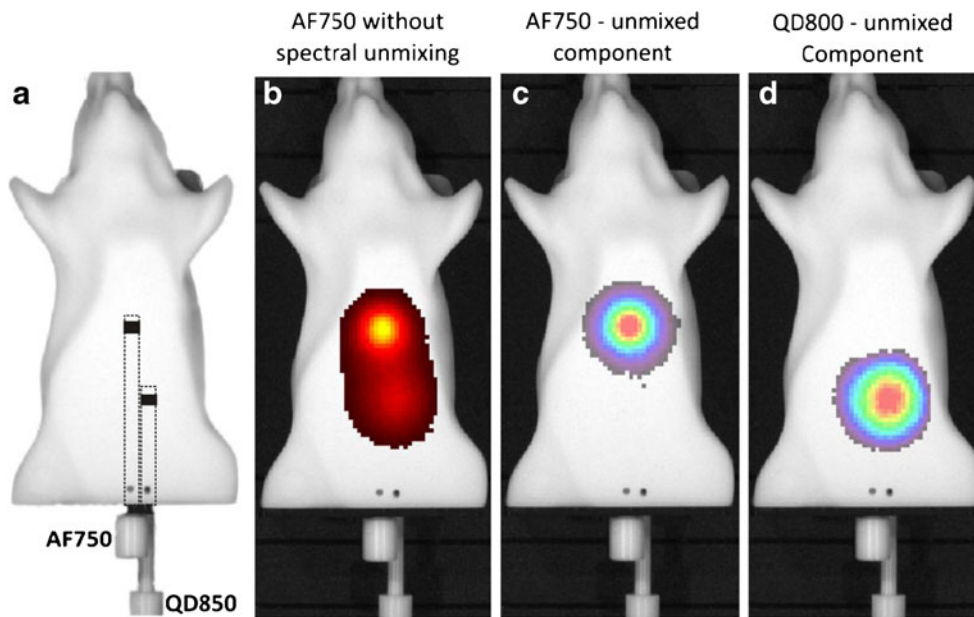


Fig. 4 Separate imaging of two fluorescent dyes with overlapping spectra using the spectral unmixing algorithm of the IVIS Lumina II. A phantom mouse was equipped with two rods which contained at their ends Alexa Fluor 750 (AF750) and quantum dot 850 (QD850), respectively (Scheme **a**). Image **b** was obtained at the optimal filter settings of AF750 (λ_{ex} =745 nm and λ_{em} =800 nm). Images **c** and **d**

were obtained after spectral unmixing and they respectively show the spectral unmixed AF750 component and QD850 component. Spectral unmixing was performed by combining the 605 nm, 640 nm, 675 nm, 710 nm and 745 nm excitation filters with the 820 nm emission filter. The other settings were: f/stop 2, exposure time automatically determined per filter combination by the system, binning 4×4

images were subsequently used by the spectral unmixing software to unmix the DiD-fluorescence signal from the background. The image of the mouse obtained after spectral unmixing clearly reveals four different fluorescent spots

(Fig. 5c). In contrast, without spectral unmixing, the fourth spot, containing the lowest DiD-liposome concentration, remained invisible (Fig. 5b). This demonstrates that spectral unmixing at least doubles the in vivo sensitivity.

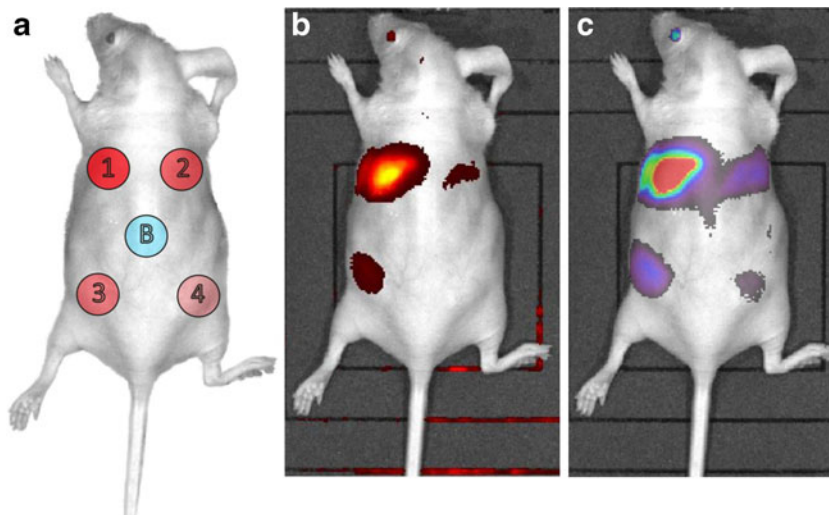


Fig. 5 Effect of spectral unmixing on the in vivo fluorescence sensitivity. Mixtures containing decreasing DiD-liposome concentrations in matrigel were subcutaneously injected in four different spots on the dorsal side. The location of these injections is shown in scheme **a**. The concentration of the DiD-liposomes in spot 1, 2, 3 and 4 were 224pM, 45pM, 11pM and 5.6pM, respectively. In spot **(b)** a mixture of buffer and matrigel was injected. Image B was generated with the IVIS Lumina II without using the spectral unmixing algorithm (settings: f/stop

stop 2, exposure time 1 s, binning 4×4 , filters λ_{ex} =640 nm/ λ_{em} =720 nm). Image C shows the DiD-liposomes in the same mouse after spectral unmixing with the IVIS Lumina II. To generate image **c**, the 640 nm excitation filter was combined with the 720 nm, 740 nm, 760 nm and 780 nm emission filters. The other measuring parameters were: f/stop 2, exposure time automatically determined per filter combination by the system, binning 4×4

Bioluminescence Imaging Capabilities

In Vitro Sensitivity

To compare the bioluminescence sensitivity of the three instruments serial dilutions of bioluminescent *E. coli* were made in a black 96-well plate. The amount of bacteria per well varied between 1.5×10^6 and 100. The 96-well plates were imaged with each instrument using the most optimal settings, mentioned in the legend of Fig. 6. As shown in Fig. 6, the lowest amount of bacteria that could be detected by the IVIS Lumina II was 1500. However, to reach this sensitivity the highest binning was needed. Due to this high binning the spatial resolution was low, which caused a fusion of the bioluminescent signals of neighbouring wells. The Photon Imager and the Image Station were less sensitive: the lowest amount of bacteria that could be detected was 1.5×10^4 and 1.5×10^5 , respectively. However, the Photon Imager generated bioluminescent spots that were nicely demarcated.

In Vivo Sensitivity and Image Quality

To evaluate whether the bioluminescence imaging capabilities of an in vivo optical imaging instrument can be estimated from in vitro experiments, we subcutaneously injected four different amounts of bacteria in separated spots on the dorsal side of a mouse. Matrigel was again used to keep the bacteria as much as possible in the injected area. A negative control consisting of a 1:1 mixture of buffer and matrigel was injected in between the four spots (Fig. 7a). The mice were imaged with the three instruments using the settings given in the legend of Fig. 7. The visible detection limit of bacteria in the Photon Imager and the Image Station was 1.125×10^4 and 1.125×10^5 CFU. In agreement with the in vitro data (Fig. 6) the IVIS Lumina II was also the most sensitive instrument in

vivo and allowed the detection of 1125 CFU. Again, a high binning was needed to reach this high sensitivity which made the bioluminescent spots obtained with the IVIS Lumina II diffuse. By digitally smoothing the images afterwards, making them appear as if they were obtained using lower binning, better quality images could be obtained.

Discussion

The enormous success of in vivo optical imaging techniques in fundamental pre-clinical research is accompanied by a drastic increase in the number of companies that develop and offer these systems. For research groups planning to purchase such a system, it is not always easy to decide which system suits their needs best. This article aims to aid them in their search for the most appropriate in vivo optical imaging system capable of both fluorescence and bioluminescence imaging. We compared three state of the art systems: the IVIS Lumina II (CaliperLS, USA), the Photon Imager (Biospace, France) and the Image Station (Kodak, USA). Other in vivo optical imaging systems have recently been compared [18, 19]. We evaluated the performance of the systems by examining their sensitivity in vitro and in vivo for both 2D bioluminescent and fluorescent imaging. The comparison was done side-by-side to exclude differences between systems arising from variations in sample preparation, injection volume or mice. Additionally, the added value of spectral unmixing algorithms for in vivo optical imaging systems was studied. All measurements were performed at the most optimal settings of each system. These settings, which included exposure time, f/stop, binning, emission and excitation filters, were selected in agreement with the companies' optical imaging experts. If one studies these settings it is remarkable that the selected filters by the expert of CaliperLS do not perfectly fit the theoretical

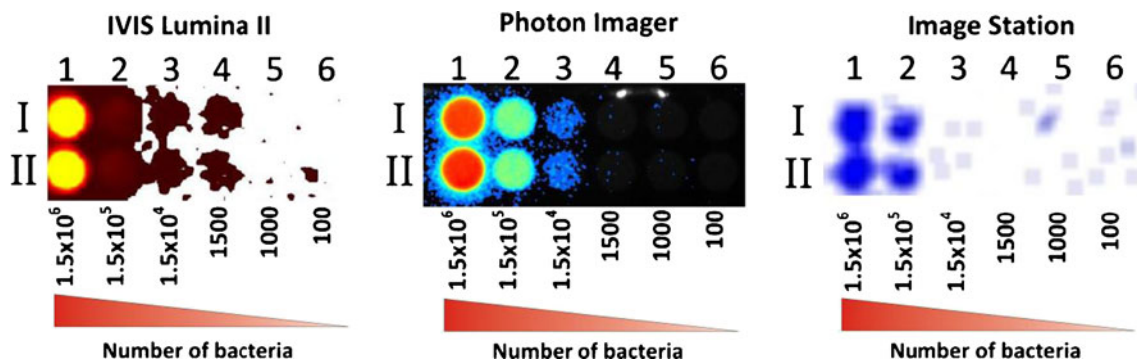


Fig. 6 In vitro bioluminescence sensitivity of the optical imaging systems. Two serial dilutions of bioluminescent *Escherichia coli* were prepared in 96-well plates (rows I and II) and imaged with the three systems. The bacterial concentration in each row decreased from left to right. The images of the bioluminescent bacteria were taken using the

following settings; *IVIS Lumina II*: f/stop 1, exposure time 300 s, binning 16×16 (to reduce the spot size we changed the binning to 1×1 after the image was taken) *Photon Imager*: f/stop 1.4, exposure time 301 s; *Image Station*: f/stop 2.51, exposure time 180 s, binning 16×16

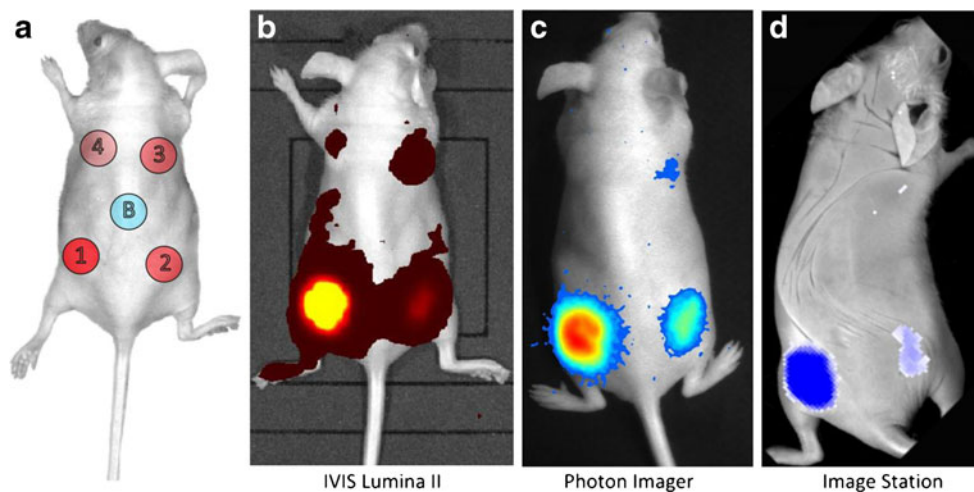


Fig. 7 In vivo bioluminescence sensitivity and image quality of the tested optical imaging systems. Decreasing amounts of bioluminescent bacteria mixed with matrigel were subcutaneously injected in four different spots on the dorsal side. The location of these injections is shown in scheme **a**. The number of bacteria in spot 1, 2, 3 and 4 are 1.125×10^6 , 1.125×10^5 , 1.125×10^4 and 1125 respectively. In spot **(b)** a

mixture of buffer and matrigel was injected. Images **B**, **C** and **D** show the same mouse imaged by the three evaluated systems. Image were taken using the following settings; *IVIS Lumina II*: f/stop 1, exposure time 300 s, binning 8×8 ; *Photon Imager*: f/stop 1.6, exposure time 307 s; *Image Station*: f/stop 2.51, exposure time 360 s, binning 16×16

spectra of the dyes. This was an intentional choice as it is their experience that dyes show a red shift in vivo.

To evaluate the FLI capacities of the systems we used liposomes with a composition similar to the commercially available doxorubicine liposomes (Doxil®) [20]. These liposomes were labelled with DiD and DiR because their excitation/emission spectra are optimal for in vivo optical imaging (Fig. 1). Indeed, light with a wavelength below ~ 600 nm is strongly absorbed by endogenous chromophores, e.g. haemoglobin and melanin. Additionally, light is also scattered by tissues and this scattering decreases with increasing wavelength. Light with a wavelength above 900 nm however, is strongly absorbed by the water in the tissues. Therefore, the optimal window for optical imaging in vivo is between ~ 600 nm and 900 nm - also called the “optical window”. From the FLI experiments we can conclude that all systems can detect minute quantities of labeled liposomes. The Image Station, however, is the most sensitive system as the lowest visible DiD- and DiR-liposome concentration in 96-well plates is respectively 4 pM and 34 pM, whereas in the others systems, the visible detection limit of these fluorescent liposomes is respectively 11 pM and 100 pM. The higher exposure time (1 min instead of seconds in the other systems) used to generate the image may explain its higher sensitivity. On the other hand, longer exposure times on the other instruments resulted in a higher background fluorescence. When studying the images of the 96 well plates obtained with the Photon Imager, one can notice that the area of the fluorescent spots in the wells with the lowest concentrations were highly variable and often covered only a small portion of the wells. An inhomogeneous exposure of the wells to the excitation light is most

likely responsible for this observation. DiD-liposomes are more easily detected than DiR-liposomes which might be due to the higher fluorescence quantum yield of DiD (0.33 versus 0.28 for DiR in MeOH) [21] and the fact that the quantum efficiency of the CCD cameras present in the three systems is lower in the near infrared region. One would expect that, due to tissue scattering and absorption, a certain fluorophore concentration is harder to detect in vivo than in vitro, however, we did not observe this in our in vivo experiments. Indeed, with the IVIS Lumina II and the Photon Imager we found that the lowest detectable concentration of DiD-liposomes in mice was slightly lower as in 96-well plates (i.e. 5.6 pM). The fact that the excitation and emission spectrum of DiD-liposomes falls in the optical window for in vivo optical imaging cannot completely explain this observation. We believe that the following reason might be responsible for this observation. Light coming from a well of a 96-well plate is only detected through the opening on the top of the well, which has a surface of only 0.32 cm^2 . Upon subcutaneous injection, DiD-liposomes are expected to spread out over an area that is much larger than the surface of a well of a 96-well plate. This larger surface will facilitate the excitation of the dyes and subsequent detection of emission light. These phenomena probably compensate for the attenuation of excitation and emission light by tissues.

The autofluorescence of tissues is a major hurdle for in vivo fluorescence imaging. This is especially the case when dyes are used that do not fluoresce in the optical window. Additionally, when one wants to use multiple fluorophores, i.e. multiplexing, it is sometimes difficult to find fluorescent dyes that do not have overlapping spectra. In these cases,

spectral unmixing can offer a solution. Spectral unmixing makes use of a mathematical algorithm that finds the signal distribution and the pure spectrum of each component [17]. Spectral unmixing is available on both the IVIS Lumina II and Image Station. The software of the Image Station was a beta-version in which the excitation based spectral unmixing allows the user to separate different fluorochromes out of a mixture. Due to the beta-status of the Image Station's spectral unmixing software, the IVIS Lumina II spectral unmixing algorithm was intensively used as proof of concept. By running an excitation and/or emission filter scan, the spectral unmixing algorithm, based on the multivariate curve resolution method, allows for separation of the different spectral components and visualization of their distribution [17]. We evaluated the spectral unmixing algorithm using Alexa Fluor 750 (AF750) and Quantum dots 850 (QD850). Both dyes have similar emission spectra and due to the broad excitation peak of QD850, it is not possible to image AF750 separately. Indeed, when using the appropriate filter settings for AF750, QD850 will also be measured. Through spectral unmixing we were able to distinguish between AF750 and QD850. Additionally, we demonstrate that spectral unmixing can at least double the in vivo sensitivity of an in vivo optical imaging system. Similar results could be obtained with the Image Station's unmixing algorithms. Weak fluorescence signals with intensities near the auto-fluorescence of the animal were difficult to detect in the past. Nowadays however, it is possible to filter out the autofluorescence present in every single pixel of an image via spectral unmixing. This is possible due to the fact that the spectral unmixing algorithm constructs excitation or emission spectra of the different fluorescent sources, including the autofluorescence, present in the animal. To construct these spectral signatures, images taken at different excitation/emission filter combinations have to be loaded in the software. Additionally, to assist the software, the number of expected fluorescent sources can be fixed.

As mentioned, the number of available excitation and emission filters and their properties are of major importance for fluorescence imaging. The IVIS Lumina II is standard equipped with 10 excitations filter with a bandpass of 35 nm and a standard filter wheel that holds four emission filters with a rather broad bandpass as well. With these standard filter sets, spectral unmixing is not recommended. Therefore, additional filter wheels containing emission filters with a narrow bandpass (20 nm) are optionally available. However, these filter wheels are preconfigured and can only hold seven emission filters. Therefore, if for example a mouse contains dyes that have to be imaged with emission filters on separate filter wheels one must replace the wheel while the animal is present on the stage. To change the emission filter wheel in the IVIS Lumina II one has to open the imaging chamber and unscrew the holder. Therefore,

changing filter wheels during an ongoing experiment is not practical. However, it is possible to customize a filter wheels by putting in the desired individual emission filters. In the mean time, the Image Station from Kodak offers an excitation filter wheel with 28 filters with a narrow bandpass of 10 nm. Different emission filters between 420 nm and 850 nm are available with a bandpass of 35 nm, or different filters upon customer request. The amount of emission filters the system can hold is limited to four at any given time. However, changing emission filters is very easy. Due to the fact that the Image Station used excitation-based unmixing, there is no need to change these filters once the system is set up. The Photon Imager is equipped with linear spectral excitation filters (400 nm–800 nm) which allows one to select an excitation filter with a bandpass of 20 nm, every 5 nm. A limited number of emission filters (i.e. six) are present. Nevertheless, other filters are available upon special request. It is important to mention that the Photon Imager makes use of high-pass emission filters, which makes it not always evident to use multiple dyes in one experiment.

To evaluate the BLI capacities of the systems we diluted luminescent *E. coli* in black 96-well plates and imaged them in all three systems. These experiments showed that the IVIS Lumina II is the most sensitive system for BLI, as the lowest detectable number of bacteria in 96-well plates was 1500 CFU. The Photon Imager and the Image Station were respectively at least 2 and 10-fold less sensitive. BLI of the subcutaneously injected bioluminescent bacteria showed a similar trend. It is important to note that the high sensitivity of the IVIS Lumina II can only be reached when the highest binning was applied. Due to this high binning the spatial resolution of the IVIS lumina II was very low, which caused a fusion of neighbouring bioluminescent signals. The lower sensitivity of the Image Station in BLI might be due to the fact that the amount of light produced by a bioluminescent source is in general much lower than that produced by a fluorescent source. Therefore, BLI typically requires longer exposure times, which also results in a larger noise accumulation in the Image Station. Additionally, the amount of light that can reach the CCD camera of the IVIS Lumina II is, due to the low *f*/stop of the lens (maximally *f*/0.95), about 2.3 and 4-fold higher than in the Photon Imager (maximally *f*/1.4) and Image Station (maximally *f*/2), respectively.

The systems have different ways of illumination and different types of lamps which have different light outputs. Each system also shows its images in different units. It is therefore difficult to compare the images quantitatively so the different images are not set to a similar scale and are compared qualitatively, as each image shows as much signal as possible without background.

When comparing peripheral hardware, all systems are equipped with an integrated gas anesthesia system and a

catheter port. The IVIS Lumina II and Photon Imager use a different system than the Image Station to support the body temperature of the animals. The former two systems use a heated stage, which is digitally controlled. Contrary, the animals in the Image Station are placed in a transparent closed box to which heated air flows around the body, covering the entire animal. Gas anesthesia is administered through a nose cone.

Finally, it is important to mention that the Image Station can be upgraded to also acquire radioisotope-based signals beside fluorescence and luminescence. CaliperLS also provides an X-ray integrated module system, while Biospace have a different system for X-ray imaging. However, in the latter, fusion of these images is, due to the usage of different pathways labor intensive and sometimes misses accuracy.

An advantage of the Image Station and Photon Imager is its flexibility. For example, it is possible to buy a basic BLI instrument that can be upgraded afterwards with the fluorescence module. Recently, Biospace lab also launched an ‘in actio module’ which makes it possible to image fluorescent and bioluminescent light in real time in non-sedated animals. This is possible because of the intensifier tube, which elevates the signal far above any dark-current background. Indeed, systems that employ a cooled CCD have a higher read out noise in the first few seconds of measuring, making real-time imaging difficult. Shortly after the introduction of the in actio module, CaliperLS presented their IVIS kinetic which is also able to perform real time optical imaging in non-sedated animals. IVIS kinetics contains a fast electron multiplying CCD. The Photon Imager and the IVIS Lumina II can also be equipped with an additional macrolens which makes it possible to acquire images at a higher magnification. The Image Station has an integrated zoom lens which allows one to obtain a higher magnification.

Conclusion

From this side-by-side comparison we can conclude that the IVIS Lumina II is the most sensitive system for bioluminescence imaging. The Photon Imager was a close second, while the Image Station was at least 10-fold less sensitive than the IVIS Lumina II. For fluorescence imaging, the three systems were quite comparable. The Kodak Image Station was slightly more sensitive than the other two systems in vitro. However, in vivo, the fluorescence sensitivity of the three systems was comparable. Spectral unmixing algorithms have recently been introduced in in vivo optical imaging. Here we demonstrated that spectral unmixing not only enables the separate imaging of dyes with overlapping spectra, but also doubles the in vivo sensitivity and thus allows for the detection of lower signals. Both the IVIS Lumina II and Image Station can perform spectral unmixing,

although the spectral unmixing software from CaliperLS was, at the time of the evaluation, more elaborate and easier to use. The results of this side-by-side evaluation and the technical comparison of the tested in vivo optical systems will be of great help for those research groups that plan to invest in in vivo optical imaging. Moreover, the work may also be of importance for researchers who want to learn more about in vivo optical imaging.

Acknowledgements We would like to thank the companies for lending us their demo optical imaging system for thorough testing. We would also like to thank their representatives for sharing their knowledge about their systems and in vivo optical imaging.

We acknowledge funding support from EU (FP7 project “SonoDrugs”), FWO (grant n° G.0621.10) and Bijzonder Onderzoeksfonds (BOF) from the Ghent University.

Conflict of Interests At the time of experimentation, no system had been bought by the Laboratory for Gene Therapy, nor were negotiations ongoing with any of the companies.

References

1. Chamberland D, Jiang YB, Wang XD (2010) Optical imaging: new tools for arthritis. *Integr Biol-Uk* 2(10):496–509
2. Licha K, Olbrich C (2005) Optical imaging in drug discovery and diagnostic applications. *Adv Drug Deliv Rev* 57(8):1087–1108
3. Stanga PE, Lim JJ, Hamilton P (2003) Indocyanine green angiography in chorioretinal diseases: Indications and interpretation: an evidence-based update. *Ophthalmology* 110(1):15–21, quiz 22–13
4. Zhang C, Liu T, Su YP, Luo SL, Zhu Y, Tan X, Fan S, Zhang LL, Zhou Y, Cheng TM, Shi CM (2010) A near-infrared fluorescent heptamethine indocyanine dye with preferential tumor accumulation for in vivo imaging. *Biomaterials* 31(25):6612–6617
5. Foucault ML, Thomas L, Goussard S, Branchini BR, Grillot-Courvalin C (2010) In vivo bioluminescence imaging for the study of intestinal colonization by *Escherichia coli* in mice. *Appl Environ Microbiol* 76(1):264–274
6. Kim JB, Urban K, Cochran E, Lee S, Ang A, Rice B, Bata A, Campbell K, Coffee R, Gorodinsky A, Lu Z, Zhou H, Kishimoto TK, Lassota P (2010) Non-invasive detection of a small number of bioluminescent cancer cells in vivo. *PLoS One* 5(2)
7. Rabinovich BA, Ye Y, Etto T, Chen JQ, Levitsky HI, Overwijk WW, Cooper LNJ, Gelovani J, Hwu P (2008) Visualizing fewer than 10 mouse T cells with an enhanced firefly luciferase in immunocompetent mouse models of cancer. *Proc Natl Acad Sci U S A* 105(38):14342–14346
8. Contag PR (2002) Whole-animal cellular and molecular imaging to accelerate drug development. *Drug Discov Today* 7(10):555–562
9. Dufort S, Sancey L, Wenk C, Jossier V, Coll JL (2010) Optical small animal imaging in the drug discovery process. *Bba-Biomembranes* 1798(12):2266–2273
10. Edinger M, Cao YA, Hornig YS, Jenkins DE, Verneris MR, Bachmann MH, Negrin RS, Contag CH (2002) Advancing animal models of neoplasia through in vivo bioluminescence imaging. *Eur J Cancer* 38(16):2128–2136
11. Ye X, Li Y, Stawicki S, Couto S, Eastham-Anderson J, Kallop D, Weimer R, Wu Y, Pei L (2010) An anti-Axl monoclonal antibody attenuates xenograft tumor growth and enhances the

- effect of multiple anticancer therapies. *Oncogene* 29(38):5254–5264
12. Baker AM, Cox TR, Bird D, Lang G, Murray GI, Sun XF, Southall SM, Wilson JR, Erler JT (2011) The Role of Lysyl Oxidase in SRC-Dependent Proliferation and Metastasis of Colorectal Cancer. *J Natl Cancer Inst* 103(5):407–424
 13. Pleijhuis RG, Langhout GC, Helfrich W, Themelis G, Sarantopoulos A, Crane LM, Harlaar NJ, de Jong JS, Ntziachristos V, van Dam GM (2011) Near-infrared fluorescence (NIRF) imaging in breast-conserving surgery: assessing intraoperative techniques in tissue-simulating breast phantoms. *Eur J Surg Oncol* 37(1):32–39
 14. Kagadis GC, Loudos G, Katsanos K, Langer SG, Nikiforidis GC (2010) In vivo small animal imaging: current status and future prospects. *Med Phys* 37(12):6421–6442
 15. Shu XK, Royant A, Lin MZ, Aguilera TA, Lev-Ram V, Steinbach PA, Tsien RY (2009) Mammalian Expression of Infrared Fluorescent Proteins Engineered from a Bacterial Phytochrome. *Science* 324(5928):804–807
 16. Deliolanis NC, Kasmieh R, Wurdinger T, Tannous BA, Shah K, Ntziachristos V (2008) Performance of the red-shifted fluorescent proteins in deep-tissue molecular imaging applications. *J Biomed Opt* 13(4):044008
 17. Xu H, Rice BW (2009) In-vivo fluorescence imaging with a multivariate curve resolution spectral unmixing technique. *J Biomed Opt* 14(6):064011
 18. de la Zerda A, Bodapati S, Teed R, Schipper ML, Keren S, Smith BR, Ng JST, Gambhir SS (2010) A comparison between time domain and spectral imaging systems for imaging quantum dots in small living animals. *Mol Imaging Biol* 12(5):500–508
 19. Keren S, Gheysens O, Levin CS, Gambhir SS (2008) A comparison between a time domain and continuous wave small animal optical imaging system. *IEEE Trans Med Imaging* 27(1):58–63
 20. Lentacker I, Geers B, Demeester J, De Smedt SC, Sanders NN (2010) Design and Evaluation of Doxorubicin-containing Microbubbles for Ultrasound-triggered Doxorubicin Delivery: Cytotoxicity and Mechanisms Involved. *Mol Ther* 18(1):101–108
 21. Texier I, Goutayer M, Da Silva A, Guyon L, Djaker N, Josserand V, Neumann E, Bibette J, Vinet F (2009) Cyanine-loaded lipid nanoparticles for improved in vivo fluorescence imaging. *J Biomed Opt* 14(5)